

# Complex low-frequency dielectric relaxation of the charge-density wave state in the $(2,5(\text{OCH}_3)_2\text{DCNQI})_2\text{Li}$

M. Pinterić<sup>1,2</sup>, T. Vuletić<sup>1</sup>, S. Tomić<sup>1</sup>, and J.U. von Schütz<sup>3</sup>

<sup>1</sup> Institute of Physics, P.O. Box 304, HR-10001 Zagreb (Croatia)

<sup>2</sup> Faculty of Civil Engineering, University of Maribor, SLO-2000 Maribor (Slovenia)

<sup>3</sup> 3. Physikalisches Institut, Universität Stuttgart, D-70550 Stuttgart (Germany)

Received: date / Revised version: date

**Abstract.** We report a detailed characterization of an unique 2- and 4-fold commensurate charge density wave (CDW) state in single crystals of the organic conductor  $(2,5(\text{OCH}_3)_2\text{DCNQI})_2\text{Li}$  by means of low-frequency (0.1 Hz–1 MHz) dielectric spectroscopy. We show that in addition to the narrow Debye-like relaxation mode of strength  $\Delta\varepsilon \approx 10^7$  with Arrhenius-like resistive decay, associated with long wavelength phason excitations, a new mode of weaker strength  $\Delta\varepsilon \approx 10^6$  appears below 40 K and broadens with decrease in temperature. Below 25 K the mean relaxation time of the new mode saturates, whereas the Debye mode continues gradual slowing down with weaker temperature dependence, again similar to the DC conductivity. We attribute the new process to short wavelength CDW excitations that become dominant once the free carrier density is substantially reduced at low temperatures.

**PACS.** 72.15.Nj Collective modes, low dimensional conductors – 71.45.Lr Charge density wave systems – 77.22.Gm Dielectric loss and relaxation

## 1 Introduction

The low-frequency dielectric response of the pinned charge and spin density waves (abbreviated as DW) has been the subject of an important number of studies in the last 15 years. The response is characterized by dielectric constants of the order  $10^6$ – $10^9$ , and is broader than the Debye one which is expected for the system with a single degree of freedom [1–4]. The dielectric function is usually described by expressions like Havriliak-Negami or Cole-Cole that imply the existence of broad distribution of time scales. This feature is associated with a single process due to a distribution of metastable states around the equilibrium position. These metastable states correspond to local changes of the phase of the pinned DW in a random defect potential. With decreasing temperature, as long as free carrier excitations are present, the time scales rapidly shift to low frequencies with the rate defined by free carrier activation energy. Whereas the main properties of DW dynamics at high temperatures are well understood, there is a number of intriguing properties at low temperatures that remain unexplained. Once the free carrier density becomes smaller than the one electron per phason characteristic length, a crossover from the thermally activated behaviour to a more smooth temperature dependence has been observed and taken as an indication that the resistive dissipation mechanism becomes unimportant at lower

temperatures [5, 6]. In the case of  $(\text{TMTSF})_2\text{PF}_6$  we have shown that, in this low temperature region, the relaxation is governed by low energy barriers two times smaller than the free carrier activation energy [7]. In addition, it has been argued that the lack of resistive dissipation is in origin of a saturated, temperature-independent behaviour of the relaxation time observed recently in the commensurate spin density wave (SDW) and charge density wave (CDW) state of  $\kappa$ -(BEDT-TTF)<sub>2</sub>Cu[N(CN)<sub>2</sub>]Cl [8] and deuterated DCNQI<sub>2</sub>Cu systems [9], respectively. In both latter cases, DW responds to the outer AC perturbation field by its short wavelength excitations associated with domain walls in respective commensurate structures.

$(2,5(\text{OCH}_3)_2\text{DCNQI})_2\text{Li}$  (abbreviated as DCNQI<sub>2</sub>Li) represents a model system of DCNQI<sub>2</sub>X (X=Li or Ag) group of compounds [10] that stand apart from others DW systems because of an coexistence of two commensurate CDW with different orders of commensurability  $N = 2$  and  $N = 4$ . One-dimensional  $N = 2$  and  $N = 4$  CDW fluctuations start to grow up below RT and 100 K, respectively, and the phase transitions are placed at  $T_{C1}(N = 2) \approx 60$  K and  $T_{C2}(N = 4) \approx 50$  K. We have already reported [11] complex conductivity measurements between 20 Hz and 1 MHz in the low temperature CDW state over the temperature range 25 K and 75 K. These measurements revealed a strong Debye-like relaxation of the charge-density wave phase mode with Arrhenius-like decay determined by the resistive dissipation. We have

proposed that at the origin of the observed relaxation are phason long wavelength excitations of  $N = 4$  CDW pinned by commensurability to the lattice via coexistent  $N = 2$  CDW.

However, some particular properties of the high ( $T > 25$  K) and low temperature ( $T < 25$  K) regions, like (i) different temperature dependence of the conductivity at low electric fields and (ii) different shape of current-voltage characteristics, and a sharp increase of the threshold field ( $E_T$ ) for non-linear conduction below 25 K followed by a concomitant decrease of the non-linear contribution, required more attention [12]. Clearly, an extension of the dielectric studies to temperatures below 25 K has seemed highly desirable. An additional motivation is the interesting question of the CDW dielectric response in the limit of ineffective screening due to a negligible free carrier density that is realized in the low temperature region below 25 K in this system [12].

To address these issues, we have undertaken a new investigation of the CDW state in the DCNQI<sub>2</sub>Li system at frequencies between 0.1 Hz and 1 MHz over the temperature range 6 K and 75 K. The present study confirms the main qualitative features of the Debye mode at temperatures higher than 25 K, and enables to track the dielectric relaxation to lower temperatures and frequencies than reported before. Moreover, this study shows that the low-frequency dielectric relaxation is more complex than we had considered. The high resolution dielectric function analysis in the complex plane [8,9] applied to measured data uncovers an additional broad mode centred at several orders of magnitude higher frequencies at low temperatures than rapidly slowing down Debye mode.

## 2 Experimental and results

The single crystals of (2,5(OCH<sub>3</sub>)<sub>2</sub>DCNQI)<sub>2</sub>Li used in this study were between 1 and 7 mm long, and had cross-sections  $10^{-3}$ – $10^{-4}$  mm<sup>2</sup>. Four-probe DC measurements indicated that the contact resistance was always much less than sample resistance. Furthermore, at low frequencies both four-probe and two-probe configurations were used with identical results. In order to cover a large frequency range, two different methods were used to measure the complex conductivity ( $G(\omega)$ ,  $B(\omega)$ ). At high frequencies (20 Hz–1 MHz) a Hewlett Packard HP4284A impedance analyser was used. At low frequencies (0.1 Hz–3 kHz) a set-up for measuring high-impedance samples was used. The AC voltage from a Tabor 8023 arbitrary function generator is applied to sample. The current response of sample is transformed to the voltage by a Stanford Research current preamplifier SR570, and subsequently detected by a Stanford Research dual-channel lock-in amplifier SR830. We point out that we obtained the same results by using both methods in the frequency range 20 Hz–3 kHz where these methods overlap. Concerning AC signal levels, we have employed the same amplitudes as in our first study [11]. Further, we have assured, by taking into account the results of open-circuit measurements, that the stray capacitances do not influence the real part of the

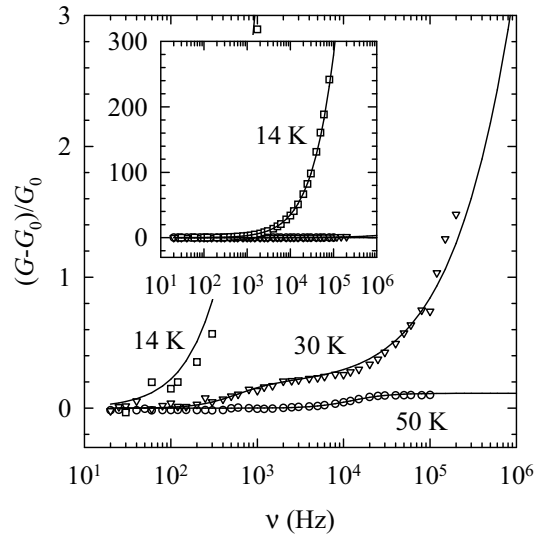


**Fig. 1.** Sample 1: Real part of the conductivity normalised to the DC value  $(G - G_0)/G_0$  versus frequency for three selected temperatures. Full lines are fits to the HN forms.

conductivity in the frequency window 0.1 Hz–1 MHz and in the temperature range of our study. This procedure removes background influences and improves sensitivity of the measurement. Measured data were analyzed by using the least squared method in the complex plane [8, 9]. This approach that takes into consideration both real and imaginary part of the dielectric function at the same time strongly improves the resolution if compared with the method we used before [11], in which the real and imaginary parts are treated separately. This method proved itself to be a powerful tool to resolve reliably two close modes in frequency even if the dielectric strength of one or both modes does not exceed 300, providing that their dielectric strengths differ less than two orders of magnitude.

On slow cooling the resistance of samples displayed already reported behaviour [11–13]. In what follows we will first present results obtained in the frequency window 20 Hz–1 MHz. Eight different single crystals were measured and all exhibited qualitatively the same behaviour. We will show results for the crystal studied in the most detail and we will refer to it as sample 1 throughout the paper. At the end of this section, we will show results observed for single crystal, referred to as sample 2, in the frequency range 0.1 Hz–1 MHz.

The real part of the conductivity normalised to the DC value  $(G(\nu) - G_0)/G_0$ , as a function of frequency at three selected temperatures is shown in Figure 1.  $G_0$  is the DC conductivity obtained from the  $G(\omega)$  measured at low frequencies where  $G(\omega)$  was independent of  $\omega$  ( $\omega = 2\pi\nu$ ). Dielectric functions were extracted from the conductivity using the relations  $\varepsilon'(\omega) = B(\omega)/\omega$  and  $\varepsilon''(\omega) = (G(\omega) - G_0)/\omega$ . Figure 2 shows frequency domain plots of the real and imaginary parts of the dielectric function for three representative temperatures. The calculated Cole-Cole plots are presented in Figure 3. The observed dielectric response can be well fitted by the phenomeno-

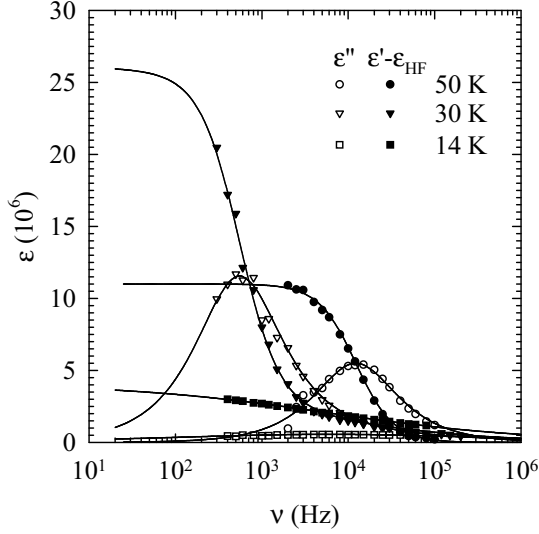


**Fig. 2.** Sample 1: Frequency dependence (log scale) of the real and imaginary parts of the dielectric function for three representative temperatures. Full lines are fits to the HN forms.

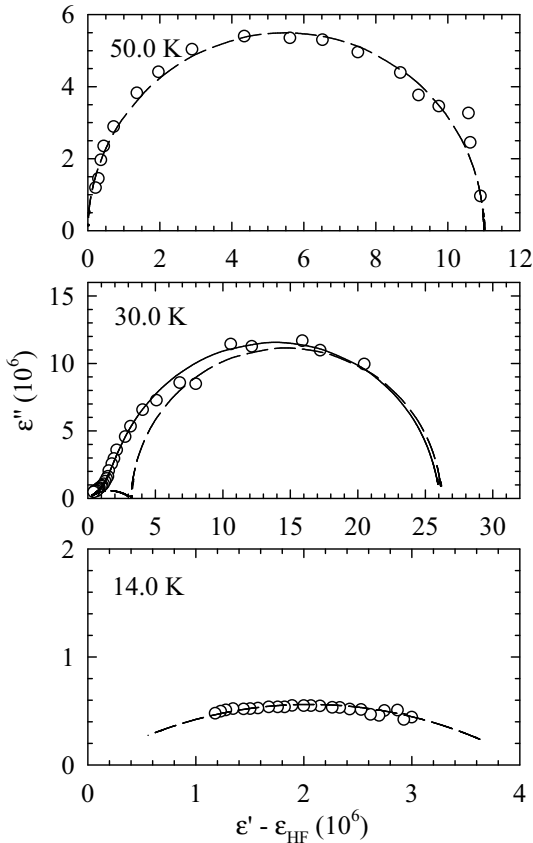


**Fig. 3.** Sample 1: Cole-Cole plots of the dielectric response at three selected temperatures. Dashed lines and full lines are fits to the single HN form and to the sum of the two HN forms, respectively.

logical Havriliak-Negami (HN) function widely used to describe relaxation processes in disordered systems [14]

$$\varepsilon(\omega) - \varepsilon_{\text{HF}} = \frac{\Delta\varepsilon}{1 + (i\omega\tau_0)^{1-\alpha}} \quad (1)$$

$\Delta\varepsilon = \varepsilon_0 - \varepsilon_{\text{HF}}$  is the relaxation strength, and  $\varepsilon_0$  and  $\varepsilon_{\text{HF}}$  are the static and the high frequency dielectric constant, respectively.  $\tau_0$  and  $1 - \alpha$  are the mean relaxation time and the shape parameter which describes the symmetric broadening of the relaxation time distribution function, respectively. While the observed dielectric response in the frequency window 100 Hz–1 MHz, was successfully fitted to a single HN mode at temperatures higher than 40 K and lower than 25 K, similar attempts to fit the data in the intermediate temperature range  $25 \text{ K} < T < 40 \text{ K}$  failed. Therefore, the obvious solution was to try to fit the observed data to a formula representing a sum of two HN modes. The full lines in Figures 1 and 2 correspond to the calculated fits to one, or sum of the two HN functions, as required. In Figure 3 every arc designated by dashed line represents a single dielectric mode, whereas the arc at 30 K drawn by full line represent the sum of the two dielectric modes. The intersection of the arcs with  $\varepsilon' - \varepsilon_{\text{HF}}$  axis at high  $\varepsilon' - \varepsilon_{\text{HF}}$  values, corresponding to low frequencies, indicates the value of the relaxation strength  $\Delta\varepsilon = \varepsilon_0 - \varepsilon_{\text{HF}}$ .  $\varepsilon_{\text{HF}}$  was found to correspond to the value of stray capacitance obtained in the “open-circuit” measurements, indicating that the intrinsic  $\varepsilon_{\text{HF}}$  of sample is negligible compared to its  $\varepsilon_0$  value. In addition to the already reported Debye mode with  $\Delta\varepsilon$  of the order of  $10^7$ , there is an additional mode centred at higher frequencies with one order of magnitude smaller strength  $\Delta\varepsilon \approx 10^6$  found at temperatures lower than 40 K. A representative complex relaxation at 30 K is displayed in Figures 1, 2 and 3.

The fit parameters as a function of inverse temperature are shown in Figure 4. Open circles stand for the Debye mode already reported before, and full circles stand for a new mode observed in this study for the first time. We will refer to these modes as the high temperature (HT) and the low temperature (LT) mode, respectively. The three parameters, that is the strength of the relaxation process  $\Delta\varepsilon$ , the width of the relaxation time distribution expressed by the  $1 - \alpha$  parameter and the mean relaxation time  $\tau_0$ , which fully characterize the HT relaxation process show the values and the temperature dependence as found earlier [11].  $\Delta\varepsilon$  of the LT mode is an order of magnitude weaker ( $\Delta\varepsilon \approx 10^6$ ) and also does not change with temperature. The  $1 - \alpha$  parameter is close to 1 at 40 K. However, already below 35 K the mode broadens and  $1 - \alpha$  attains values as small as 0.35 below about 25 K. The  $\tau_0$  parameter displays an almost temperature independent behaviour below 25 K. On the other hand, it is difficult to determine the temperature dependence of the relaxation time above 25 K. The reason for this is that the relatively weak LT mode is cornered between the upper limit of frequency window and the HT mode, causing a relatively large scatter in  $\tau_0$  values in  $25 \text{ K} < T < 40 \text{ K}$  range.

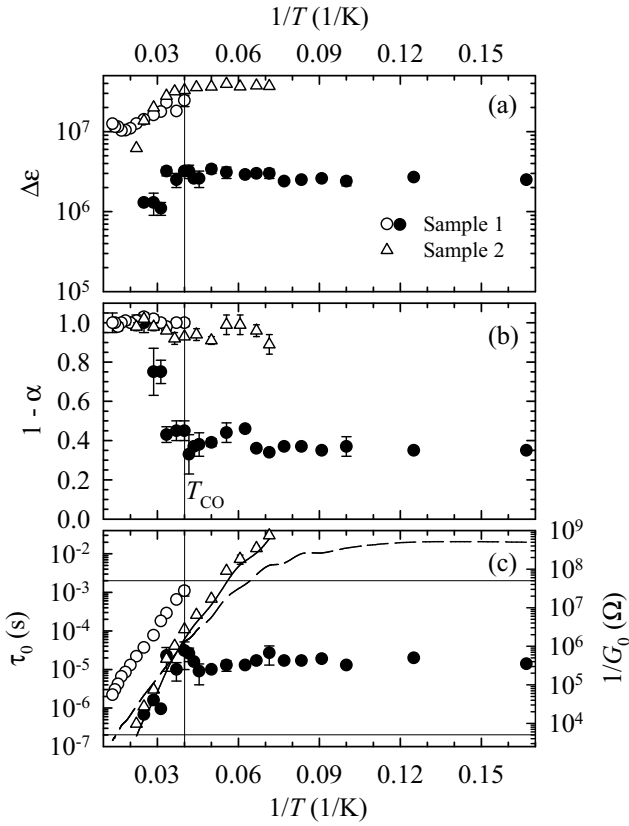


**Fig. 4.** (a) Relaxation strength ( $\Delta\varepsilon$ ), (b) shape parameter ( $1-\alpha$ ) and (c) mean relaxation time ( $\tau_0$ ) versus inverse temperature. Open and full circles for the HT and the LT relaxation mode observed for sample 1, respectively. Triangles show the HT mode observed for sample 2. Dashed and full line represent the associated DC resistance ( $1/G_0$ ) behaviour for sample 1 and sample 2, respectively. Vertical lines in panel (c) designate the experimental frequency window for sample 1.

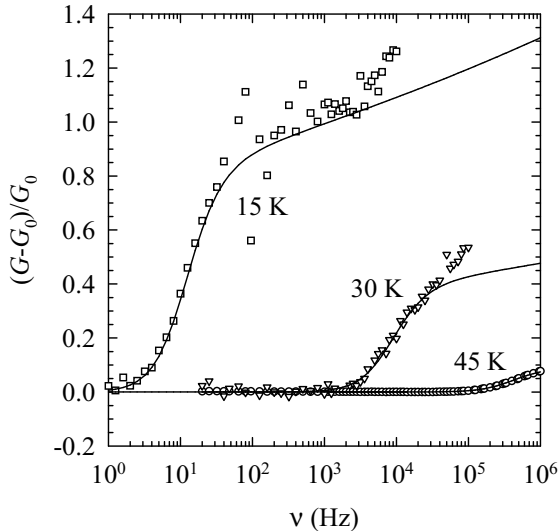


**Fig. 5.** Sample 2: Real part of the conductivity normalized to the DC value  $(G - G_0)/G_0$  versus frequency for three selected temperatures. Full lines are fits to the HN form.

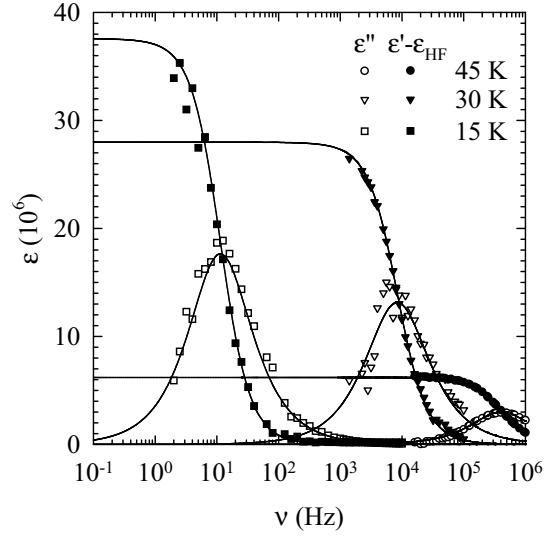


**Fig. 6.** Sample 2: Frequency dependence (log scale) of the real and imaginary parts of the dielectric function for three representative temperatures. Full lines are fits to the HN form.

In addition, we show the HT mode (labelled by triangles in Figure 4) observed for sample 2 and tracked down to frequencies as low as 0.1 Hz. The real part of the conductivity as a function of frequency and the dielectric function as a function of frequency are displayed in Figures 5 and 6, respectively. It should be noted that the magnitudes and the temperature behaviour of the  $\Delta\varepsilon$  and  $(1-\alpha)$  parameters are the same as observed for sample 1. Moreover, the mean relaxation time is found to follow the temperature behaviour of the DC conductivity also at temperatures lower than 25 K. However, the HT mode in sample 2 is found to be shifted by 1.5 decades to higher frequencies. For example, at 40 K the HT mode is centred at 140 kHz in comparison to 4 kHz in sample 1. Further, the LT mode was not observed in our frequency window. However, it should be noted that the intrinsic  $\varepsilon_{\text{HF}}$  of sample 2 was found to be substantial  $\varepsilon_{\text{HF}} \approx 4 \times 10^6$ , in contrast to the negligible  $\varepsilon_{\text{HF}}$  found in sample 1 in which both HT and LT modes were observed. The large high frequency dielectric constant indicates an additional relaxation strength situated in the frequency range of a few MHz. Again, this value is above our available frequency range. Keeping in mind that the LT mode is centred at about 1.5 orders of magnitude higher frequencies than the HT one, the large intrinsic  $\varepsilon_{\text{HF}}$  should be assigned to the missing LT mode. Indeed, it should be noted that the value of  $\varepsilon_{\text{HF}} \approx 4 \times 10^6$  corresponds well to the relaxation strength  $\Delta\varepsilon$  of the LT mode found in sample 1 (see Figure 4).

Finally, we note that our investigation covered eight single crystals of various synthesis, differing in respective values of the relaxation frequency  $(2\pi\tau_0)^{-1}$  for several orders of magnitude. The position of the LT mode was always found to be at 1.5–3 decades higher frequencies than the HT one. For two single crystals, as represented by sample 2, the LT mode was not observed inside our frequency window due to a relatively high  $(2\pi\tau_0)^{-1}$  of the HT mode.

Further, a scatter observed in the activation energy for the relaxation time ( $320 \pm 60$  K) and the magnitude of dielectric strength ( $(3 \pm 2) \times 10^7$ ) cannot be correlated with the observed difference in  $\tau_0$ . A smaller  $\tau_0$  would indicate a higher impurity level in sample 2. However, in the framework of the classical picture of CDW pinning [3,4], it is difficult to reconcile this finding with a negligible effect of impurities on the strength of dielectric relaxation. Therefore, it is clear that the standard theoretical model is by far insufficient to provide an adequate theoretical picture for the complex relaxation of density waves at low frequencies and low temperatures in real materials. We propose that subtle variations of the disorder level in nominally pure samples might be responsible for the observed differences in relaxation times.

### 3 Discussion

The observed dielectric properties of (2,5(OCH<sub>3</sub>)<sub>2</sub>DCNQI)<sub>2</sub>Li reveal the existence of two relaxation processes that we have assigned to as the high temperature and the low temperature process. We had discussed the origin and the nature of the HT process in detail in our previous communication (see [11]). In short, we have argued, on the basis of a huge  $\Delta\varepsilon$  and a Debye form, that the HT process might be attributed to the phason mode of  $N = 4$  CDW pinned by commensurability to the underlying lattice due to the coexistence of  $N = 2$  CDW. The interaction with free carriers has been identified as the dominant dissipation mechanism in the temperature region down to 25 K, since the response of CDW was found to gradually slow down with an activation energy equal to the free carrier activation energy  $\Delta \approx \Delta_{fc} \approx 320$  K. Our new data confirm these findings and show that at  $T < 25$  K the HT process continues to slow down and eventually disappears from the experimental frequency window below 14 K. In Figure 4(c) a crossover at about 25 K, that separates high and low temperature region with different activation energy is clearly visible. Above 25 K the temperature dependence of DC resistivity is well described by an Arrhenius behaviour with free-carrier activation energy of 320 K. However, below 25 K the resistance obviously starts to level off. In the low temperature region we can either fit the data to the Arrhenius behaviour with a two times smaller activation energy of about 170 K, or to the Mott's variable range hopping (VRH) formula as we have done before [12,13]. Both fits give equally good results down to about 14 K. A new process assigned to as the LT process, emerges at 40 K in our frequency window. Below 25 K, the LT mode moves extremely slowly and remains inside our experimental frequency window down to 6 K. The temperature of 25 K reveals itself clearly as the crossover temperature  $T_{CO}$  for both HT and LT relaxation processes. We have already proposed to identify  $T_{CO} \approx 25$  K as the temperature below which the linear electron density becomes smaller than the one electron per CDW characteristic length  $L_{DW}$  [12]. This condition appears to be satisfied at  $T < T_{CO} \approx 25$  K on

the basis of the following consideration. Namely, knowing that the one-electron length  $l_e$  at high temperatures is about  $8 \times 10^{-4} \mu\text{m}$  and taking into account the resistance rise of about three orders of magnitude down to 25 K, we get  $l_e$  to be about  $1 \mu\text{m}$  at that temperature. On the other hand, in order to get an estimate for  $L_{DW}$ , we use the theoretical expression developed by K. Maki that relates Fukuyama-Lee-Rice (FLR) length ( $L_{DW}$ ) with the corresponding threshold field for non-linear conduction [15–18]. Taking the value of  $E_T$  obtained in our measurements (see [12]), we get  $L_{DW}$  to be about  $1 \mu\text{m}$  at 25 K. We point out that no direct determination of FLR length, using X-ray diffraction or dark field transmission electron microscopy, has been done for DCNQI<sub>2</sub>Li material until now. However, we would like to note that the value of  $1 \mu\text{m}$  corresponds well to those observed in other CDW systems [19]. It is worth of noting that available theoretical models also expect that  $L_{DW}$  along chains values to 1–10  $\mu\text{m}$  [20].

In what follows, we are going to address more in detail the CDW dynamics in the low temperature region, *i.e.* at  $T < T_{CO} \approx 25$  K. In order to do that, we find useful to show representative temperature domain plots of the real part of dielectric function. The plots of  $\varepsilon'$  as a function of temperature for the selected choice of frequencies are shown in Figure 7 (a) and (b) for the HT and the LT process, respectively. As far as  $\varepsilon'$  *versus*  $T$  for the HT process is concerned, two features should be noted. First is that  $\varepsilon'$  starts to decrease with temperature below  $\omega\tau_0 = 1$  line. That is, at temperatures where the mean relaxation time is larger than the duration of AC perturbation, the DW ceases gradually to be able to follow the AC perturbation and the dielectric function decreases [5,7,21]. Second feature concerns the behaviour of  $\varepsilon'$  below  $\omega\tau_0 = 1$  line. Two distinct dissipation regimes, above and below the crossover temperature  $T_{CO}$ , are reflected in the behaviour of  $\varepsilon'$

$$\varepsilon'(T) \propto \varepsilon' e^{-\Delta/T} \quad (2)$$

At  $T_{CO} < T < T_C$  and  $14 \text{ K} < T < T_{CO}$  CDW dynamics is governed by free carrier activation energy  $\Delta \approx \Delta_{fc} \approx 320$  K and by low energy barriers  $\Delta \approx 0.5\Delta_{fc} \approx 170$  K, respectively. Therefore, it should be noted that, as far as the HT process is concerned, the dielectric response (both  $\varepsilon'$  and  $\tau_0$ ) as well as the DC conductivity are governed by the same energy barriers down to about 14 K. Two possible explanations for smaller activation rate in the range  $14 \text{ K} < T < T_{CO}$  might be envisaged. First is the existence of an anisotropic quasi-particle energy gap [22], which would imply that the phason long wavelength excitations remain to be present also below crossover temperature  $T_{CO} \approx 25$  K. The second possibility is that the phason excitations are frozen and replaced by solitons or domain walls, which are short wavelength CDW excitations. We recall that the soliton's excitation energy in the quasi-one-dimensional system like polyacetylene is about 0.6 of the quasi-particle activation energy [23,24], similarly as we find in DCNQI<sub>2</sub>Li system.

As far as the LT process is concerned, we note that  $\omega\tau_0 = 1$  line does not appear to play a role as in the

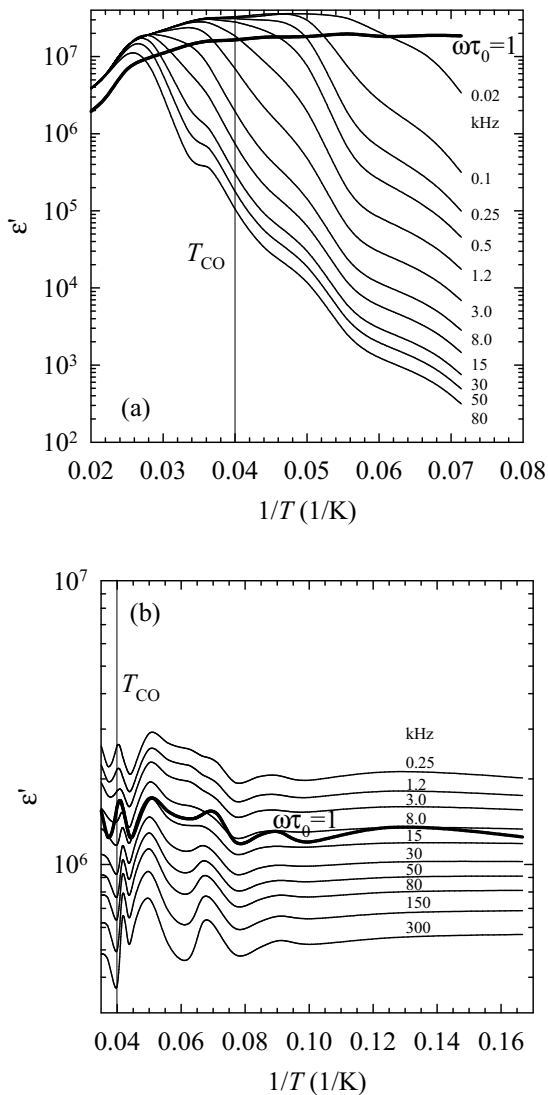


**Fig. 7.** Real part of the dielectric function *versus* inverse temperature for (a) HT and (b) LT dielectric mode at a few selected frequencies. A noise in  $\epsilon'$  is due to the scatter in values of  $1 - \alpha$  parameter.

case of the HT process. At  $T < T_{CO}$  the relaxation is governed by very low energy barriers of the order of a few Kelvin. A qualitatively similar behaviour has been recently observed in the dielectric response of commensurate DW in  $\kappa$ -(BEDT-TTF)<sub>2</sub>Cu[N(CN)<sub>2</sub>]Cl [8] and deuterated DCNQI<sub>2</sub>Cu systems [9], in which the free carrier screening has been found to be insignificant as for the LT process. Furthermore, in the temperature range between 40 K and 14 K, the LT process, in contrast to the HT process, is not governed by the same energy barriers as the DC conductivity. Conversely, below about 14 K the DC conductivity levels off in agreement with the almost temperature independent behaviour of the LT mode. The former behaviour indicates that excitations responsible for the LT process are different than those responsible for the HT one. At this stage it might be useful to look at the information about the low temperature state of CDW, we can get from our

ESR measurements [25]. That is, our pulsed ESR data below 30 K show a considerable freezing of both electronic motion and spin exchange. The degeneracy of electronic relaxation times  $T_1$  and  $T_2$  is lifted below 30 K, the ESR lines become in-homogeneously broadened and exhibit a Curie-like susceptibility. Such spin behaviour can be described in the framework of REHAC model [26], which implies that spin pairing occurs leading to domains with zero spin. The random domain structure at low temperatures appear, in this model, as a natural consequence of the strong charge and spin localization, *i.e.* it is due to the absence of the free carrier screening. Remaining spins ( $s = \frac{1}{2}$ ), which might be naturally associated to topological defects, are exchange coupled weakly via these domains. Susceptibility considerations give an upper limit for the length of these domains of about 100 lattice units, which amounts to  $0.05 \mu\text{m}$ . Therefore, we are lead to propose that these domains of  $0.05 \mu\text{m}$  size might be attributed to the entities responsible for the LT process, which becomes a dominant CDW relaxation at very low temperatures.

Finally, we would like to comment the electric-field dependent conductivity in the crossover region. We recall that, below 25 K, the shape of current-voltage characteristics changes, the threshold field ( $E_T$ ) for non-linear conduction starts to increase sharply, and concomitantly the non-linear contribution starts to diminish [12]. These features might be interpreted as a sign of gradual freezing of the high temperature sliding mechanism, which is theoretically due to the coupling of the phason mode to a DC field. In the framework of the single-particle model for DW, which predicts  $\Delta\epsilon \cdot E_T = \text{const}$ , a strong increase of  $E_T$  implies that the dielectric strength of the HT mode should concomitantly vanish. The latter would indicate that the Arrhenius-like relaxation with  $\Delta \approx 0.5\Delta_{fc}$  at  $T < 25$  K is only a low-temperature branch of the HT process. However, our available experimental data cannot confirm the existence of another mode, which critically slows down in the temperature range between 40 K–6 K. In addition, it should be noted that the dielectric strength of the HT mode, after an initial slight increase, keeps a constant value at least down to 14 K. Nevertheless, it is worth of noting that such a scenario of the CDW dynamics has been recently established in the CDW state of the inorganic compound o-TaS<sub>3</sub> [6,27–29]. That is, whereas the high temperature phason mode critically slows down, two new modes, attributed to topological defects, emerge below  $T_{CO}$  that is about 50 K in this compound. Moreover, the latter modes show qualitatively similar slow temperature dependence as the HT and the LT modes in DCNQI<sub>2</sub>Li at  $T < T_{CO} \approx 25$  K. In addition, it is worth of mentioning that  $T_{CO} \approx 25$  K corresponds closely to  $0.5T_C$ , where  $T_C$  is the phase transition temperature at which  $N = 4$  CDW is established. It has been already noticed by Monceau *et al.* [30] that the contribution of short wavelength excitations due to local CDW deformations become visible below about  $0.5T_C \approx T_{CO}$ . This assertion would also imply that CDW excitations associated with the HT process, as well as to the DC conductivity,

at  $T < 25$  K should be attributed to topological defects. At lower temperatures novel strongly localized DW excitations associated with the LT process start to contribute to the DC conductivity at high, as well as at low fields, and eventually become dominant excitations below about 14 K.

## 4 Conclusion

In conclusion, our low frequency dielectric measurements have identified, for the first time, that two length and time scales are involved in the low temperature dynamics of the charge-density wave state of (2,5(OCH<sub>3</sub>)<sub>2</sub>DCNQI)<sub>2</sub>Li. We identify the strong Debye relaxation of the  $N = 4$  CDW pinned by commensurability with Arrhenius-like decay as the high temperature process, and the long wavelength phason excitations as the relaxation entity. At temperatures at which the free carrier screening is effective ( $T > T_{CO} \approx 25$  K), the CDW dynamics is governed by the free carrier activation energy  $\Delta_{fc}$ . Conversely, at  $T < T_{CO}$  the system is brought into metastable states with low energy barriers of about  $0.5\Delta_{fc}$ . Concomitantly, an order of magnitude weaker mode with a broad distribution of relaxation times centred at 1.5 decades higher frequency emerges and gradually prevails over. We attribute this low temperature mode to short wavelength CDW excitations associated with topological defects. The estimated size of these entities is about  $0.05 \mu\text{m}$ , and associated energy barriers are of the order of a few Kelvin.

Finally, more work is needed to be done to elucidate the nature of relaxation entities associated with the HT process at  $T < T_{CO}$ . In addition, further measurements and analysis are under way in order to reveal the temperature behaviour of the LT mode at  $T > T_{CO}$ .

We thank Kazumi Maki for valuable discussions. A participation of Neven Biškup in the early stage of this work is acknowledged. This work was partially supported by Croatia-Germany bilateral collaboration project, reference KRO-005-98.

## References

1. R. J. Cava, R. M. Fleming, P. Littlewood, E. A. Rietman, L. F. Schneemeyer, and R. G. Dunn, *Phys. Rev. B* **30**(6), 3228 (1984).
2. P. B. Littlewood, *Phys. Rev. B* **36**(6), 3108 (1987).
3. G. Grüner, *Rev. Mod. Phys.* **60**(4), 1129 (1988).
4. G. Grüner, *Rev. Mod. Phys.* **66**(1), 1 (1994).
5. S. Tomić, N. Biškup, and A. Omerzu, *Synth. Met.* **85**, 1597 (1997).
6. K. Biljaković, D. Starešinić, K. Hosseini, W. Brütting, H. Berger, and F. Lévy, *Physica B* **244**, 167 (1998).
7. S. Tomić, M. Pinterić, T. Vuletić, J. U. von Schütz, and D. Schweitzer, *Synth. Met.* **120**, 695 (2001).
8. M. Pinterić, M. Miljak, N. Biškup, O. Milat, I. Aviani, S. Tomić, D. Schweitzer, W. Strunz, and I. Heinen, *Eur. Phys. J. B* **11**(2), 217 (1999).
9. M. Pinterić, T. Vuletić, M. Lončarić, S. Tomić, and J. U. von Schütz, *Eur. Phys. J. B* **16**(3), 487 (2000).
10. P. Erk, S. Hünig, J. U. von Schütz, H.-P. Werner, H. C. Wolf, D. Jérôme, S. Tomić, R. T. Henriques, and D. Schmeißer, in *Organic Superconductivity*, edited by V. Z. Kresin and W. A. Little (Plenum Press, New York, 1991), pp. 325–334, ISBN 0-306-43730-9.
11. S. Tomić, N. Biškup, M. Pinterić, J. U. von Schütz, H. Schmitt, and R. Moret, *Europhys. Lett.* **38**(3), 219 (1997).
12. M. Pinterić, N. Biškup, S. Tomić, and J. U. von Schütz, *Synth. Met.* **103**, 2185 (1999).
13. M. Pinterić, S. Tomić, and J. U. von Schütz, in *34th International Conference on Microelectronics, Devices and Materials with the Satellite Minisymposium on Semiconductor Radiation Detectors, September 23. - 25. 1998, Rogaška Slatina, Slovenia. Proceedings*, edited by M. Hrovat, D. Križaj, and I. Šorli (MIDEM - Society for Microelectronics, Electronic Components and Materials, Ljubljana, 1998), pp. 99–104, ISBN 961-90001-6-1.
14. S. Havriliak and S. Negami, *J. Polym. Sci. C* **8**, 161 (1967).
15. A. Bjeliš and K. Maki, *Phys. Rev. B* **44**(13), 6799 (1991).
16. K. Maki and A. Virosztek, *Phys. Rev. B* **42**(1), 655 (1990).
17. K. Maki and A. Virosztek, *J. Magn. Magn. Mater.* **90–91**, 758 (1990).
18. K. Maki, in *Microscopic Aspects of Nonlinearity in Condensed Matter*, edited by A. R. Bishop, V. L. Pokrovsky, and V. Tognetti (Plenum Press, New York, 1992), pp. 147–158, ISBN 0-306-44001-6.
19. C. H. Chen and R. M. Fleming, *Solid State Commun.* **48**(9), 777 (1983).
20. J. R. Tucker, W. G. Lyons, and G. Gammie, *Phys. Rev. B* **38**(2), 1148 (1988).
21. J. C. Lasjaunias, K. Biljaković, F. Nad', P. Monceau, and K. Bechgaard, *Phys. Rev. Lett.* **72**(8), 1283 (1994).
22. B. Dóra and A. Virosztek, *J. Phys. IV France* **9**(10), Pr10 (1999).
23. W. P. Su, J. R. Schrieffer, and A. J. Heeger, *Phys. Rev. Lett.* **42**(25), 1698 (1979).
24. H. Takayama, Y. R. Lin-Liu, and K. Maki, *Phys. Rev. B* **21**(6), 2388 (1980).
25. W. Bietsch, J. U. von Schütz, and H. C. Wolf, *Appl. Magn. Reson.* **7**(2–3), 271 (1994).
26. L. C. Tippie and W. G. Clark, *Phys. Rev. B* **23**(11), 5846 (1981).
27. K. Biljaković, D. Starešinić, K. Hosseini, and W. Brütting, *Synth. Met.* **103**, 2616 (1999).
28. D. Starešinić, *Contribution to the Investigation of Low Energy Excitations in Quasi One-Dimensional Systems*, Ph.D. thesis, Université Joseph Fourier, Grenoble and University of Zagreb (2000).
29. D. Starešinić *et al.* (to be published).
30. P. Monceau and F. Ya. Nad', *Synth. Met.* **70**, 1255 (1995).